Transportation Research Part E 171 (2023) 103036

Contents lists available at ScienceDirect

Transportation Research Part E

journal homepage: www.elsevier.com/locate/tre

Experience-based territory planning and driver assignment with predicted demand and driver present condition

Yifu Li [a,1], Chenhao Zhou [b,*,1], Peixue Yuan [b,1], Thi Tu Anh Ngo [c]

[a] International Institute of Finance, School of Management, University of Science and Technology of China, Hefei 230026, China
[b] School of Management, Northwestern Polytechnical University, Xi'an 710072, China
[c] Department of Industrial Systems Engineering and Management, National University of Singapore, Singapore

ARTICLE INFO

Keywords:
Territory planning
Driver assignment
Learning effect
Rolling horizon method
Markov decision process

ABSTRACT

The parcel delivery industry has enjoyed rapid growth with the rise of the e-commerce business. To survive the highly competitive market, service providers have introduced various methods to improve the customer experience, for example, providing faster response or wider delivery coverage. One way is to adopt the territory-based delivery system, in which each courier serves a fixed group of customers. In this study, we propose a novel territory design method allowing the territory plan to be adjusted while guaranteeing service consistency. The territory planning problem (TPP) can be formulated as a Markov decision process (MDP), and we develop a two-stage Rolling Horizon (TSRH) method to compute the optimal territory plan. In the first stage, the algorithm assigns certain cells to the drivers based on the predicted demands. In the second stage, the remaining cells are assigned to the drivers with the actual demands while taking driver experience into consideration. The computational studies reveal that the proposed TSRH method is able to resolve the TPP efficiently, and it is robust under different situations. The TSRH method outperforms the classical method with fixed core areas. We also find that the learning potential and learning efficiency can largely impact the optimal territory plan, which eventually leads to significant improvement on driver's performance.

1. Introduction

With the rise of e-commerce business and technological advances, the parcel delivery industry has enjoyed rapid growth in the past decades. Various last-mile delivery companies emerge in the period, and the competition soon becomes severe. To survive in the highly competitive market, the service providers have switched from business-oriented to customer-oriented, in which the customer experience is treated as a significant factor in the service (Karmarkar, 2015). With such changes in the business model, the service providers are working hard to improve the service quality, for example, faster response, wider delivery converge, and longer service time. Both the big firms and new venture companies have realized the importance of customer experience in the delivery service, and treated it as an influential element to distinguish their service from the others.

The service providers have adopted both the new technologies and new delivery systems to improve the service experience. First, novel technologies like package stations and express cabinets are adopted. The Cainiao station[2] is a type of local logistic

* Corresponding author.
E-mail addresses: yifuli@ustc.edu.cn (Y. Li), zhouchenhao@nwpu.edu.cn (C. Zhou).
[1] First three authors contribute equally.
[2] https://www.cainiao.com/school.html.

https://doi.org/10.1016/j.tre.2023.103036
Received 20 March 2022; Received in revised form 17 December 2022; Accepted 25 January 2023
Available online 7 February 2023
1366-5545/

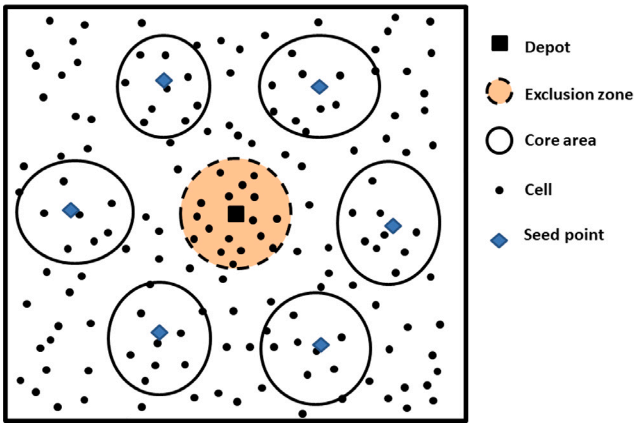

Fig. 1. Routing concepts in Zhong et al. (2007).

facility operating by the Alibaba Group, which offers mail, storing, and collecting services. The Honeycomb express cabinet[3] is a fully automated cabinet, which has been widely installed in neighborhoods in China. The customers can mail or collect the parcels with the express cabinet by interacting with the control panel on their own. Delivery to the package station and express cabinet has become the mainstream form of package delivery in China, which enhances both delivery efficiency and customer satisfaction, and the door-to-door service only works for bulky packages or special items. The application of the package station and express cabinet has freed both the customers and the couriers from the time window constraints, such that they can deliver and collect at their convenient time. In addition, it allows the drivers to use trucks to conduct the consolidated delivery to the station or cabinet, which increases the capacity of the drivers.

Second, service providers have developed different delivery systems to enhance the service quality. One way is to assign the same driver to the same set of customers regularly (e.g., Groër et al., 2009), which allows him to use personal knowledge to serve his customers better. In the practice of package delivery, the service provider no longer provides a detailed routing plan for the drivers, but just assigns the delivery tasks to the drivers. The drivers can make the routing plans based on their experience (e.g., acknowledgment of shortcuts and locations in the service territory), which reduces the delivery time, and they can also adjust the plan at any time when emergencies like traffic jams occur, or when the customer is unavailable for a moment of time (Chang and Yen, 2012; Quirion-Blais and Chen, 2021). Owning to the fixed driver delivery mode, the bond between driver and customer is also strengthened, which improves customer loyalty, and enhances the repurchasing of the service (Smilowitz et al., 2013).

In this paper, we focus on designing a vehicle dispatching system considering the changes in logistics technologies, and benefits of driver familiarity. The vehicle dispatching problem is stochastic: (i) The demands of the customers vary every day; (ii) Past dispatching plans can have an impact on future decisions because the delivery experience can affect driver's delivery efficiency. The vehicle dispatching problem can be considered as a stochastic vehicle routing problem, and Laporte (1992) has shown it is difficult to be resolved, even by the heuristic algorithm. One way to tackle the dispatching problem is to treat it as a TPP and adopt a territory-based delivery system, which divides the service region into several territories to be served by the couriers (drivers) (e.g., Wong and Beasley, 1984; Beasley, 1984). Without optimizing vehicle routes and schedules, the territory-based method focuses on area allocation to the drivers, which significantly reduces the size of the search space.

The classical territory-based methods are efficient in solving the dispatching problem, but they are suggested to have little routing flexibility, because the service region of a driver is fixed. To resolve the problem, some researchers discard the procedure of territory partition, but treat it as a consistent vehicle routing problem, in which a customer must be served by the same driver (e.g., Groër et al., 2009; Kovacs et al., 2015). The others introduce a TPP with adjustable territories. For example, Zhong et al. (2007) propose a two-stage territory design algorithm. They introduce the concepts of "cell", "core area", "flex zone", and "seed point". Fig. 1 illustrates these routing concepts, and we present the definitions in Appendix A. Only the core areas are fixed in Zhong et al. (2007), and the service provider can adjust the daily delivery plan by assigning the cells outside the exclusion zone and core areas to the drivers. Later on, Schneider et al. (2014) introduce a modular territory routing method, which also has two stages. They apply the algorithm to the vehicle routing problem with time window constraints and investigate the performance of the algorithm. Recently, Bender et al. (2016) introduce a multi-period service territory design problem. They divide the TPP into two subproblems: The customer partition subproblem and the worker scheduling problem. They introduce a location–allocation heuristic algorithm to resolve the worker scheduling subproblem.

This study also considers a territory-based delivery system, which offers seasonal or annual vehicle dispatching plans. We assume that the drivers are able to use trucks to conduct the delivery to the package stations, and hence the vehicle capacity constraint is no longer considered. We formulate the TPP as an MDP, because its stochastic properties. The TPP is suggested to be NP-hard (Zhong

[3] https://www.fcbox.com/en/pc/index.html.

et al., 2007; Schneider et al., 2014). Different from the literature focus on identifying delivery policies analytically (e.g., Cook and Lodree, 2017), our paper aims to develop algorithms to resolve the TPP. We introduce a TSRH algorithm, which is under the framework of the Rolling Horizon method. The TSRH algorithm differs from Zhong et al. (2007) and Schneider et al. (2014) in the following aspects: (i) The TSRH algorithm adopts the periodical predicted data to mitigate the demand variances. (ii) The TSRH algorithm is in the framework of the rolling horizon method instead of tabu search, which allows the core areas to be adjusted periodically. (iii) We adopt the approximation method on the traveling time rather than compute the routing plan of each driver in the daily problem. These features allow the TSRH algorithm to make the delivery plan based on the predicted demand surge, and adjust the plans when the drivers accumulate more delivery experience. The TSRH method is proved to be efficient and robust by our computational studies, which reveals the algorithm has the potential to be used in resolving practical problems. In addition, we find that the TSRH method outperforms the two-stage territory planning (TSTP) method introduced in Zhong et al. (2007) with reduced traveling time. We further conduct several computational studies on the effects of learning parameters, which provides insights on the behavior of the drivers.

The remaining paper is organized as follows. Section 2 reviews the literature related to the territory design and vehicle routing problem with learning effect. We present the proposed MDP model in Section 3 and introduce the TSRH algorithm in Section 4. We report the numerical studies in Section 5, and conclude the paper in Section 6.

2. Literature review

Our study contributes to the literature in two major fields: territory planning and vehicle dispatching, and the transportation problems with learning effects.

2.1. Territory planning and vehicle dispatching

The literature on territory planning and vehicle dispatching focus on how to divide the service region into multiple territories the drivers handle and maximize the overall delivery efficiency. Schneider et al. (2014) provide a thorough review of the territory design problem, and Bender et al. (2016) summarize the latest advance in this area.

The idea of territory design can trace back to Wong and Beasley (1984) on the vehicle dispatching problem with fixed delivery areas. They divide the service region into several territories to be served by the drivers. The territory is divided by the historical demand data and their algorithm aggregates the customers who show up together frequently into the same territory. In a paper close to our study, Zhong et al. (2007) investigate the territory planning problem with learning effect. They introduce several routing concepts and propose a Tabu search algorithm to compute the solution. However, they do not consider using predicted demands in making territory assignment decisions. Later, Schneider et al. (2014) study the territory planning problem with time window constraints. They propose a modular territory routing method with two phases, which assign the core areas and the daily routing plans in each phase respectively. Bender et al. (2016) discuss a multi-period service territory design problem, in which each worker is responsible for the customers in his territory. They introduce a location–allocation heuristic for the worker scheduling problem. Although the above literature integrates the vehicle routing problem in the algorithm, which allows territory to be planned with better accuracy, the difficulty of solving the problem surges along with the increasing problem scales.

Researchers also investigate the approximation methods in estimating the workload of a driver in the vehicle dispatching problem. Readers are referred to Nicola et al. (2019) for a thorough review of the relevant literature. Beardwood et al. (1959) are among the first authors who study the traveling time approximation. They propose a method to estimate the travel time of the traveling salesman problem over a given region. They suggest that the traveling time is proportional to the number of stops and the area of the region. Stein (1978) calibrates the parameters in the model of Beardwood et al. (1959), and Larson and Odoni (1981) prove that the estimation converges well for the vehicle dispatching problem. Later on, the estimation method has been extended to the capacity constrained vehicle routing problem (e.g., Daganzo, 1984) and vehicle routing problem with time window (e.g., Figliozzi, 2009). Recently, Zhong et al. (2007) propose a method, which can estimate the traveling time of a driver with the distances between customer, seed point, and depot. Dong and Turnquist (2015) discuss an approximation method to the supplier shipping problem with vehicle routing and delivery frequency decisions. In our study, we adopt the approximation method rather than solving the vehicle routing problem for a driver. We apply the method proposed by Daganzo (1984), Figliozzi (2009) and Zhong et al. (2007) in estimating the travel time of inter-cell and intra-cell transportation respectively.

Recent studies on territory design and vehicle dispatching include Zhang et al. (2011) on the urban drayage operation optimization problem with Rolling Horizon method, Huang et al. (2018) on a 2-echelon logistic system design problem with pickup and delivery, Lee et al. (2021) on the territory-based flexible bus dispatching problem, Pei et al. (2021) on the vehicle dispatching problem with modular vehicle technologies, Lespay and Suchan (2022) on the multi-period vehicle routing algorithm, and Sandoval et al. (2022) on the districting design problem in the last mile delivery. Our work advances the territory planning literature by proposing a TSRH algorithm, which (1) adopts an estimation method to derive travel time, (2) incorporates predicted data in making the territory planning decisions and (3) allows the core areas to be adjusted periodically to fit the demand variances. Service providers can apply our algorithm in making vehicle dispatching decisions in practice.

2.2. Transportation problems with learning effects

Our study also contributes to the literature on transportation problems with learning effects. Jaber (2016) and Glock et al. (2019) provide thorough reviews of models and applications on this stream of study.

There is rich literature that discusses the mathematical model of the learning effect, which links the relationship between service experience and delivery efficiency. These mathematical models are called learning curves, including log-linear model (e.g., Jaber and Glock, 2013), exponential model (e.g., De Jong, 1957), and hyperbolic model (e.g., Mazur and Hastie, 1978). In our study, we follow the exponential learning model in Chen et al. (2016), which can trace back to the learning curve proposed by De Jong (1957). We choose the model because it can depict the phenomenon that there is a certain limit of the travel time that can be compressed in the practice. Chen et al. (2016) study a technician routing problem with learning effect. They formulate the problem as an MDP and use the myopic approach to resolve the problem and study the impact of the learning effect. We also model the problem as an MDP, however, we use a Rolling Horizon method to resolve the problem, which can apply the predicted demands in computing vehicle dispatching plans.

Recent advances in this stream of literature include Hewitt et al. (2015) and Valeva et al. (2017) on workforce planning problems with learning effect, Chen et al. (2017) on the multi-period technician scheduling problem with experience-based traveling time, Zhang et al. (2019) on the online scheduling problem considering picker's learning effect for an online to offline community supermarket, Ulmer et al. (2020) on the binary driver-customer familiarity investment problem, and Kumar et al. (2021) on the supply chain coordination problem. Our paper contributes to the literature by providing a TSRH algorithm to resolve the TPP with learning effects, and analyzing the impact of learning effect on the optimal territory plan.

3. Problem formulation

In this section, we will state our assumptions and formulate the TPP in Section 3.1, discuss the learning effect in Section 3.2 and finally present the MDP model in Section 3.3.

3.1. Problem description

We consider the TPP with a single depot located in the center of a rectangular service region, with K drivers and a planning time T. Let $\mathcal{K} = \{1, 2, \dots, K\}$ denote the set of drivers, and $\mathcal{T} = \{1, 2, \dots, T\}$ denote the set of dates in the planning time. We assume that $\mathcal{K}$ is invariant in any day $t \in \mathcal{T}$, but some of the drivers may be absent occasionally, and that each driver $k \in \mathcal{K}$ has a capacity μ_k, and a given limit of workload (traveling time) b_k, where $\mu_k \le b_k$. Let M_t be the matrix of present condition with element $m_{k,t} \in \{0, 1\}$, which states driver k's present condition at day t. We assume $m_{k,t} = 1$ if he presents, and $m_{k,t} = 0$ otherwise.

We use the concept of cell as (Zhong et al., 2007), which describes a block of customers. The detailed description of the routing-related concepts is presented in Appendix A. Let $\mathcal{I} = \{1, 2, \dots, I\}$ denote the set of cells, and we assume the I cells are identical squares unified distributed in the service region. At the beginning of each day $t \in \mathcal{T}$, the service provider receives the demand of all the cells in $\mathcal{I}$. Let the demand matrix be N_t with element $n_{i,t}$, which denotes the demand of cell i on day t. Following Figliozzi (2009), it is assumed that $n'_{i,t}$ demands have some unexpected events (e.g., time-window constraints or traffic jams), and let N'_t be the demand matrix with the uncertainty events.

Let $x_{i,k,t}$ be a binary decision variable, and $x_{i,k,t} = 1$ if cell i is assigned to driver k on day t, otherwise $x_{i,k,t} = 0$. The service provider needs to decide the territory plan $\boldsymbol{x}$ to minimize the overall distance traveled for the fleet.

Throughout our study, we make the following assumptions:

(i) The number of customer requests is known at the beginning of each day.

(ii) The time window of the delivery is not explicitly considered.

(iii) Route plan is limited to deliveries only, and pick-ups are scheduled separately.

(iv) Drivers are constrained by working time rather than capacity.

(v) Vehicles begin and end each day at the same depot.

The above assumptions fit the practical delivery service in China quite well. The service provider will receive the customer's requests by the morning of each day, and the time window is usually not considered because new technologies such as package stations and express cabinets are introduced. The customer can pick up from the package station and express cabinet at any time, and the driver does not have a strict schedule for the delivery. Also, because of the application of these new technologies, drivers can use trucks to conduct the delivery, which make them have enough capacity for the delivery. The drivers have to visit the depot to collect the packages before the daily service to guarantee the service quality and check up on the tasks.

3.2. Learning effect

We consider a learning process in which a driver's delivery time (performance) is a function of the number of visits to the cell. In general, the driver may spend less time in a cell when he frequently visits this cell. Let $q_{i,k,t}$ denote the number of visits of driver k on cell i by day t. We assume that all the drivers have some basic training experience q_0 at the beginning, such that $q_{i,k,1} = q_0$ for all $i \in \mathcal{I}$ and $k \in \mathcal{K}$.

We adopt a similar learning model proposed by De Jong (1957) and Chen et al. (2016) and introduce a learning factor $\rho_{i,k,t} \in [0, 1]$ to adjust the traveling time for driver k over cell i at day t. Let $\alpha_k \in [0, 1]$ denote driver k's learning potential, which states the amount of time that can be compressed by the learning effect, and $\beta_k > 0$ denote driver k's learning efficiency, which indicates the speed of traveling time compression as the experience accumulates. The learning function is given by:

$$\rho_{i,k,t} = (1 - \alpha_k) + \alpha_k q_{i,k,t}^{-\beta_k}, i \in \mathcal{I}, k \in \mathcal{K}, t \in \mathcal{T}. \tag{1}$$

The learning process describes the reduction of traveling time as the driver gets experienced. The learning factor $\rho_{i,k,t}$ is a number that is used to adjust the traveling time estimation of a driver within a cell. It reflects the driver's familiarity with the service territory. We adopt the model of Chen et al. (2016) because the learning function accounts for both the traveling time compression by the learning effect and the fact that service or production times do not go to zero as experience grows, which fits the behavior of the drivers in the package delivery industry very well.

The learning effect affects the optimal assignment greatly when the fleet is mixed with experienced and fresh drivers. Yet, it may also affect the territory planning when the drivers are all experienced but they have different familiarity with a given region. In practice, the delivery company may rotate the drivers among different depots by practical and commercial considerations. The drivers have to work at unfamiliar territories, and the learning effect decides how fast they can adapt to the new assignments.

There are several methods to calibrate the parameters α_k and β_k. They can be estimated by examining the working time or conducting a field experiment. For example, Bailey (1989) conducts field experiments to study the learning effect. The parameters in the learning models are calibrated with the experiment data. To provide a more detailed analysis on learning and forgetting, the service designer can follow Redelmeier and Kahneman (1996) to record the instant performance of the driver and set up a performance profile. The parameters can be computed by examining the performance profile.

3.3. MDP model

In this section, we present the model of the TPP. The TPP is a stochastic decision problem, because the customer demand is stochastic, and each territory-driver assignment plan has an impact on future decisions by the learning effect. The service provider needs to assign the territories to the drivers considering the daily demand variances and past experience. A natural modeling framework of such a problem is an MDP Model as follows.

(i) States

In this problem, decisions are made at the beginning of each day. Let $t \in \mathcal{T}$ be the decision epochs, where day T is the last day in the planning time. Let $\boldsymbol{s}_t$ be the state of the system at the beginning of day t, and it captures all the information that is needed to make a dispatching decision. Let $Q_t(\boldsymbol{s}_{t-1})$ be the matrix of drivers' visit numbers at day t. For simplicity, we omit $\boldsymbol{s}_{t-1}$ and use Q_t instead when there is no ambiguity. Let $q_{i,k,t}$ defined in Section 3.2 be the element of Q_t. Thus, Q_t reflects the drivers' delivery experience indirectly, because $q_{i,k,t}$ reveals the cumulative visiting experiences of driver k over cell i. Let N_t be the matrix of the demand with element $n_{i,t}$, N_t' be the matrix of the demand with uncertainty with element $n_{i,t}'$, and M_t be the matrix of drivers' present condition with element $m_{k,t}$. Then the system state on day t is given by $\boldsymbol{s}_t = (Q_t, N_t, N_t', M_t)$.

(ii) Actions

Given state $\boldsymbol{s}_t$, an action is the territory plan $\boldsymbol{x}_t$, that serves the day t requests. Here, $\boldsymbol{x}_t$ is the matrix of decision variable at day t with element $x_{i,k,t}$ for all $i \in \mathcal{I}$ and $k \in \mathcal{K}$. Define $W_k\left(\boldsymbol{x}_t, \boldsymbol{s}_t\right)$ as the traveling time for driver k with territory plan $\boldsymbol{x}_t$ and state $\boldsymbol{s}_t$. Let b_k be the maximum traveling time for driver k. A feasible action at a given date t should satisfy the following constraints:

$$W_k\left(\boldsymbol{x}_t, \boldsymbol{s}_t\right) \le b_k, k \in \mathcal{K}, \tag{2}$$

$$\sum_{k\in\mathcal{K}} x_{i,k,t} = 1, i \in \mathcal{I}, \tag{3}$$

$$\sum_{i\in\mathcal{I}} x_{i,k,t} = 0, \text{if } m_{k,t} = 0, k \in \mathcal{K}, \tag{4}$$

$$x_{i,k,t} \in \{0,1\}, i \in \mathcal{I}, \text{and } k \in \mathcal{K}. \tag{5}$$

Constraint (2) ensures the working time of driver k to be less than b_k, and constraints (3) to (5) guarantee that all the cells are served, and the absent drivers are not assigned with any cell.

(iii) Transition Function

We consider the transition function with two parts. The first is a deterministic transition by the action selected on the day t. Given state $\boldsymbol{s}_t$, and action $\boldsymbol{x}_t$, a deterministic transition is made to post-decision state $\boldsymbol{s}_t^x$ by updating the driver's experience as:

$$q_{i,k,t+1} = q_{i,k,t} + x_{i,k,t} n_{i,t}, i \in \mathcal{I}, \text{and } k \in \mathcal{K}. \tag{6}$$

The second is a stochastic transition. The demand and driver present conditions are random variables, and there is no deterministic relationship between the demands N_t and N_{t+1}, and the present conditions M_t and M_{t+1}.

On day $t+1$, the transition is made from post-decision state $\boldsymbol{s}_t$ to pre-decision state $\boldsymbol{s}_{t+1}$ by observing new demand N_{t+1} and driver present condition M_{t+1}. In this transition, the drivers' experience remains unchanged from the post-decision state, and thus $Q_{t+1} = Q_t^x$.

(iv) Contribution Function

At decision epoch t, given state $\boldsymbol{s}_t$ and action $\boldsymbol{x}_t$, a transition from pre-decision state $\boldsymbol{s}_t$ to post-decision state $\boldsymbol{s}_t^x$ results in a contribution function:

$$c\left(\boldsymbol{s}_t, \boldsymbol{x}_t\right) = \sum_{k\in\mathcal{K}} \mathrm{E}\left[W_k\left(\boldsymbol{x}_t, \boldsymbol{s}_t\right)\right], \tag{7}$$

where $c\left(\boldsymbol{s}_t, \boldsymbol{x}_t\right)$ denotes the traveling time of the whole fleet at day t with territory plan $\boldsymbol{x}_t$ and state $\boldsymbol{s}_t$.

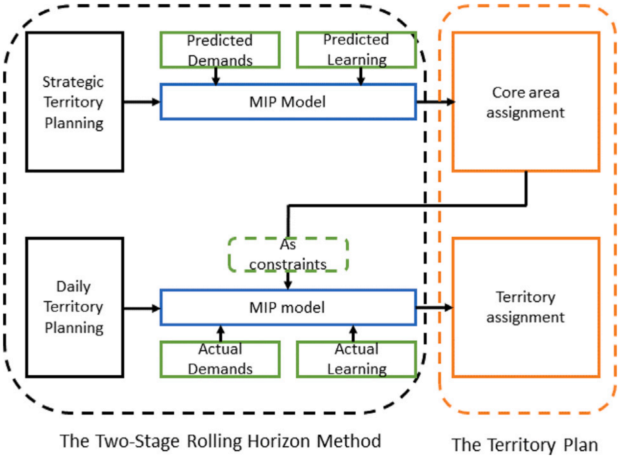

Fig. 2. The TSRH algorithm.

(v) Objective function:

The service provider seeks to minimize the overall traveling time of the drivers, and the objective of the TPP is given by:

$$\min_{x_t \in \mathcal{X}_t, \forall t \in \mathcal{T}} \mathrm{E}\left[\sum_{t \in \mathcal{T}} c\left(s_t, x_t\right)\right], \tag{8}$$

where $\mathcal{X}_t$ be the set of feasible actions (territory plans) available on day t.

The TPP is suggested to be NP-hard by Zhong et al. (2007) and Schneider et al. (2014). To resolve MDP, a common method is to solve the Bellman equation:

$$V\left(s_t\right) = \min_{x_t \in \mathcal{X}_t} \left\{c\left(s_t, x_t\right) + \mathrm{E}\left[V\left(s_{t+1}\right) | s_t, x_t\right]\right\}, \tag{9}$$

Because of the size of the state space and challenges associated with solving the Bellman equation, we propose a *TSRH algorithm*, which is presented in Section 4 to solve the TPP.

4. TSRH algorithm

In this section, we present our TSRH algorithm, which is based on the framework of the Rolling Horizon method. We use the same terms and definitions as (Zhong et al., 2007), which are presented in Appendix A, but our method differs from theirs as we allow the core areas to be adjusted with the predicted demand. Fig. 2 illustrates the framework of the proposed algorithm.

There are two stages in the TSRH algorithm: The strategic territory planning (STP) stage and the daily territory planning (DTP) stage. In the STP stage, we assign some cells to the core area of each driver. The rest cells will be assigned to the drivers in the DTP stage.

(i) STP Stage

In the STP stage, we assign the core areas with predicted demands and driver present conditions. As it is difficult to predict the demand within a short time period, we consider the demand prediction in a relatively long time period like monthly or seasonally. Different from Zhong et al. (2007), which considers fixed core area assignment, we allow the core areas to be adjusted based on the drivers' experience level.

(ii) DTP Stage

In the DTP stage, the core areas obtained in the STP stage is used as constraints, and we assign all the remaining cells to the drivers with demand realization and actual driver present conditions. We update the experience level and solve the daily cell assignment problem for the service provider.

The proposed TSRH algorithm has several advantages. First, the two-stage algorithm can reduce the computation complexity by limiting the number of cells considered in solving the problem in each stage. Thus, it has the potential to be applied in solving practical problems. Second, our algorithm can compute a territory plan based on predicted demands. This helps the service designer to be better prepared with demand variances and the spike of demands. Third, rather than solving for every state with backward dynamic programming, we can step forward in time and solve the problem with demand realization in the DTP stage, which fits the practical delivery mode and hence it is easy to be applied in practice.

In the following sections, we start by discussing the methods to estimate the workload of a driver in Section 4.1. We describe the STP problem in Section 4.2 and formulate the DTP problem in Section 4.3. Finally, we present the framework of the TSRH algorithm in Section 4.4.

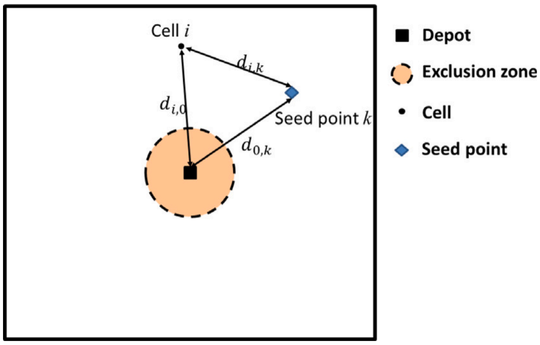

Fig. 3. An illustration of the inter-cell transportation time estimation.

4.1. Traveling time estimation

To improve the efficiency in computing the territory plan, rather than computing the travel time(i.e., the $W_k\left(\boldsymbol{x}_t, \boldsymbol{s}_t\right)$) directly, we introduce several estimation methods to approximate the travel time under a given territory plan. Similar as Zhong et al. (2007), we estimate the transportation time from two aspects: intra-cell transportation and inter-cell transportation. The intra-cell transportation depicts the delivery task of a driver within a cell, and inter-cell transportation describes the transportation time between the cells. The estimated delivery time is the sum of the intra- and inter-cell estimation time. Our estimation method approximates the traveling time with given parameters like the area of a cell and the average distance between the cells, and it reflects the actual transportation time well according to Figliozzi (2009).

(i) Intra-cell transportation

We apply an estimation method inspired by Zhong et al. (2007), Daganzo (1984) and Figliozzi (2009) to approximate the intra-cell traveling time. The intra-cell transportation time for driver k on cell i at day t with learning factor $\rho_{i,k,t}$ can be estimated by:

$$C_{i,k,t}(\rho_{i,k,t}, n_{i,t}, n'_{i,t}, \mu_k) = \rho_{i,k,t}\left(w_{1,1}\sqrt{A_i n_{i,t}} + w_{1,2}\sqrt{A_i n'_{i,t}} + w_{1,3}\frac{2\bar{d}n_{i,t}}{\mu_k}\right), \tag{10}$$

where parameters $w_{1,1}$, $w_{1,2}$, and $w_{1,3}$ are the coefficient for the traveling time estimators on intra-cell transportation, routing problem with transportation uncertainty like time window constraints or traffic congestion, and routing problem with capacity constraints. A_i is the area of cell i. $n_{i,t}$ is the actual demand of cell i at day t, and $n'_{i,t}$ is the demand with unexpected situations. $\bar{d}$ is the average distance between a cell and the seed point, and μ_k is the capacity of driver k.

Our estimation method is able to estimate the traveling time with transportation uncertainty and capacity constraints with $n'_{i,t}$ and μ_k. Parameters $w_{1,1}$, $w_{1,2}$, and $w_{1,3}$ are usually estimated by linear regression of the traveling data. Similar as Figliozzi (2009), term $w_{1,1}\sqrt{A_i n_{i,t}}$ reflects the traveling time without any practical constraint, $w_{1,2}\sqrt{A_i n'_{i,t}}$ depicts the additional traveling time introduced by transportation uncertainty such as the time-window constraints or traffic jams, and $w_{1,3}\frac{2\bar{d}n_{i,t}}{\mu_k}$ reflects the additional traveling time led by the capacity constraint of driver k.

(ii) Inter-cell transportation

We use similar method as Zhong et al. (2007) to estimate the inter-cell transportation time. The inter-cell transportation time $D_{i,k,t}(\rho_{i,k,t})$ for driver k in cell i at day t with learning factor $\rho_{i,k,t}$ can be approximated as:

$$D_{i,k,t}(\rho_{i,k,t}) = w_2\left(d_{i,k} + d_{i,0} - d_{0,k}\right)\rho_{i,k,t}, \tag{11}$$

where w_2 is a parameter for calibration. $d_{i,k}$ is the expected travel time from cell i to the seed point of core area k, $d_{i,0}$ is the expected travel time from cell i to the depot, and $d_{0,k}$ is the expected traveling time from the seed of driver k to the depot.

Fig. 3 illustrates the parameters used in the inter-cell transportation estimation. When estimating driver k's inter-cell transportation workload into cell i, the travel time $d_{i,k}, d_{i,0}$ and $d_{0,k}$ are considered, and the transportation time is affected by the learning factor $\rho_{i,k,t}$.

4.2. STP model

Based on the MDP model in Section 3.3 and the estimation methods in Section 4.1, we formulate the STP model. The TSRH algorithm resolves the STP problem every $h > 0$ days with predictions on the daily demand $\bar{N}_t$ and driver present condition $\bar{M}_t$ on day t. The service designer can apply several forecasting methods as discussed in Chopra and Meindl (2016) (e.g., Holt's model, Winter's model, moving average, and exponential smoothing) to predict the demands and present conditions based on the historical data. The STP problem uses the predicted data to compute the core area assignments. We will refer to h as the computation interval.

Let $\tau \geq 0$ be the planning period, and H be the planning horizon, where $h < H < T$. Define $\mathcal{H}_\tau = \{h\tau, h\tau+1, \ldots, \min\{h\tau+H, T\}\}$, which is the set of the dates in the planning horizon in period τ.

We compute the solution of the TPP by first solving the STP problem. Cells assigned to the core areas in the optimal solution of the STP problem will follow the same assignment in the TPP solution. Because only part of the cells can be assigned to the core areas in the STP stage, we introduce a virtual driver 0 to denote the cells not assigned to the core areas in the STP stage. Let $\mathcal{K}^+ = \{0, 1, \ldots, K\}$. The remaining cells will be assigned in the DTP stage. Let $\bar{x}_{i,k,r}$ be a binary decision variable, and $\bar{x}_{i,k,r} = 1$ if cell i is in the core area of driver k on day r, otherwise $\bar{x}_{i,k,r} = 0$. Let cell 0 denote the depot and $\mathcal{Z}$ be the set of cells in the exclusion zone. We introduce a parameter θ to adjust the minimum working time of the core area. θ can be calibrated and adjusted by the service provider based on the historical data and practical considerations. The STP problem in period h is given by:

$$\min_{\bar{\mathbf{x}}} F_1(\bar{\mathbf{x}}|\tau) = \sum_{i\in\mathcal{I}}\sum_{k\in\mathcal{K}}\sum_{r\in\mathcal{H}_\tau}\left(C_{i,k,r}(\rho_{i,k,r}, \bar{n}_{i,r}, \bar{n}'_{i,r}, \mu_k) + D_{i,k,r}(\rho_{i,k,r})\right)\bar{x}_{i,k,r}, \tag{12}$$

$$s.t.\ \sum_{i\in\mathcal{I}}\left(C_{i,k,r}(\rho_{i,k,r}, \bar{n}_{i,r}, \bar{n}'_{i,r}, \mu_k) + D_{i,k,r}(\rho_{i,k,r})\right)\bar{x}_{i,k,r} \leq b_k, k\in\mathcal{K}, \text{and } r\in\mathcal{H}_\tau, \tag{13}$$

$$\sum_{i\in\mathcal{I}}\left(C_{i,k,r}(\rho_{i,k,r}, \bar{n}_{i,r}, \bar{n}'_{i,r}, \mu_k) + D_{i,k,r}(\rho_{i,k,r})\right)\bar{x}_{i,k,r} \geq \theta b_k, k\in\mathcal{K}, \text{and } r\in\mathcal{H}_\tau, \tag{14}$$

$$\rho_{i,k,r} = (1-\alpha_k) + \alpha_k\left(\bar{q}_{i,k,r}\right)^{-\beta_k}, i\in\mathcal{I}, k\in\mathcal{K}, \text{and } r\in\mathcal{H}_\tau, \tag{15}$$

$$\bar{q}_{i,k,r+1} = \bar{q}_{i,k,r} + \bar{n}_{i,r}\bar{x}_{i,k,r}, i\in\mathcal{I}, k\in\mathcal{K}^+, \text{and } r\in\mathcal{H}_\tau, \tag{16}$$

$$\sum_{k\in\mathcal{K}}\bar{x}_{i,k,r} = 1, i\in\mathcal{I}, \text{and } r\in\mathcal{H}_\tau, \tag{17}$$

$$\bar{x}_{i,0,r} = 1, i\in\mathcal{Z}, \text{and } r\in\mathcal{H}_\tau \tag{18}$$

$$\bar{x}_{i,k,r} \in \{0,1\}, i\in\mathcal{I}, k\in\mathcal{K}^+, \text{and } r\in\mathcal{H}_\tau, \tag{19}$$

In the STP problem, constraints (13) and (14) ensures the working time of driver k is in the feasible region. Constraints (15) and (16) depict the learning process, in which the learning factor $\rho_{i,k,r}$ is updated by the service experience $q_{i,k,r}$. Finally, constraints (17) to (18) require all the customers in the service region to be served by the fleet, and there is no overlap between the territories.

We can tell from (15) that, the learning function in our study is nonlinear, which makes the problem a mixed-integer nonlinear problem (MINLP). To compute the near-optimal solution and discuss the implications, we adopt a piece-wise linear approximation method, which is presented in Appendix B. The converted mixed integer linear problem (MILP) can be resolved by the commercial MILP solvers.

4.3. DTP model

In the DTP stage, we take the core areas obtained by solving the STP problem as constraints, and assign the remaining cells to the drivers. Cells assigned in the DTP stage will follow the same assignment in the TPP solution. We compute the solution of the TPP by combining the cell assignment in the STP and DTP problems. The DTP problem on day t is given by:

$$\min_{\mathbf{x}_t} F_2(\mathbf{x}_t) = \sum_{i\in\mathcal{I}}\sum_{k\in\mathcal{K}}\left(C_{i,k,t}(\rho_{i,k,t}, n_{i,t}, n'_{i,t}, \mu_k) + D_{i,k,t}(\rho_{i,k,t})\right)x_{i,k,t}, \tag{20}$$

$$s.t.\ x_{i,k,t} \leq m_{i,k,t},\ \forall i\in\mathcal{I}, \forall k\in\mathcal{K}, \tag{21}$$

$$\sum_{i\in\mathcal{I}}\left(C_{i,k,t}(\rho_{i,k,t}, n_{i,t}, n'_{i,t}, \mu_k) + D_{i,k,t}(\rho_{i,k,t})\right)x_{i,k,t} \leq b_k,\ \forall k\in\mathcal{K}, \tag{22}$$

$$\rho_{i,k,r} = (1-\alpha_k) + \alpha_k q_{i,k,t}^{-\beta_k},\ \forall i\in\mathcal{I}, \forall k\in\mathcal{K}, \forall r\in\mathcal{H}_\tau, \tag{23}$$

$$q_{i,k,t+1} = q_{i,k,t} + n_{i,t}x_{i,k,t},\ \forall i\in\mathcal{I}, \forall k\in\mathcal{K}, \tag{24}$$

$$\sum_{k\in\mathcal{K}}x_{i,k,t} = 1,\ \forall i\in\mathcal{I}, \tag{25}$$

$$1 + x_{i,k,t} - m_{i,k,t} \geq \bar{x}_{i,k,1},\ \forall i\in\mathcal{I}, \forall k\in\mathcal{K}, \tag{26}$$

$$x_{i,k,t} \in \{0,1\}, \forall i\in\mathcal{I}, \text{ and } \forall k\in\mathcal{K}. \tag{27}$$

In the DTP problem, the cells assigned to the core areas in the STP stage are set as constraints in (26). Constraint (22) ensures the working time of driver k is in the feasible region, and constraints (23) and (24) depict the learning process. Finally, constraints (25) to (27) require all the customers in the service region to be served by the fleet, and there is no overlap between the territories. The DTP is also an MINLP. We can take the same piece-wise linear approximation method in Appendix B to convert the DTP problem into a MILP, which can be solved by the commercial solver.

4.4. Main algorithm

Based on the STP and DTP problems we formulated in Sections 4.3 and 4.4, we introduce the detailed steps of the TSRH algorithm Algorithm 1.

Algorithm 1 The TSRH algorithm

Input:
Parameters: $\mathcal{T}$, $\mathcal{K}$, $\mathcal{I}$, Q_0, $\boldsymbol{\alpha}$, $\boldsymbol{\beta}$, $\boldsymbol{b}$, $\boldsymbol{\mu}$, H, h, θ.
Output:
The optimal territory plan $\boldsymbol{x}$.

1: Initiate seed points for k core areas
2: **for** day $t = 0$ to T **do**
3:   **if** $(t \bmod h) == 0$ **then**
4:     Set $\tau = t/h$;
5:     Forecast the average daily demand $\bar{N}$, demand with uncertainty $\bar{N}'$ and driver present condition $\bar{M}$ in the future H periods, and obtain state $\bar{s}_\tau = (\bar{Q}_\tau, \bar{N}_\tau, \bar{N}'_\tau, \bar{M}_\tau)$;
6:     Solve the STP problem $F_1(\bar{\boldsymbol{x}}|\tau)$ based on state $\bar{s}_\tau$, and obtain the optimal solution $\bar{\boldsymbol{x}}^*$;
7:     Update the seed points for the k core areas;
8:   **end if**
9:   Observe demand N_t, demand with uncertainty N'_t, driver present condition M_t, and experience level Q_t at the beginning of day t;
10:   Solve DTP problem $F_2(\boldsymbol{x}, t)$ with assigned core areas $\bar{\boldsymbol{x}}^*$ as constraints, and state $\boldsymbol{s}_t = (Q_t, N_t, N'_t, M_t)$;
11:   Update driver experience level Q_{t+1} with territory plan $\boldsymbol{x}$;
12: **end for**
13: **return** $\boldsymbol{x}$.

Table 1
A summary of the numerical studies.

Section	Contents
Section 5.1	Parameter settings in the computational studies
Section 5.2	Performance of the TSRH algorithm under various situations
Section 5.3	Sensitivity analysis on the practical constraints
Section 5.4	The effects of the random error on the estimated time
Section 5.5	The effects of using the predicted demand data on the estimated time
Section 5.6	The effects of the seed point updating methods
Section 5.7	Performance comparison with the Tabu Search
Section 5.8	Territory planning with homogeneous drivers
Section 5.9	Territory planning with heterogeneous drivers

Our TSRH algorithm starts with an initialization step on selecting the initial seed points in 1. The initial seed points can be randomly generated or arbitrarily chosen by the service provider. On every h day, the algorithm updates the predicted values obtained from the provider in Step 4. Then the algorithm resolves the STP problem with the predicted value in 6 and obtains the optimal STP solution $\bar{\boldsymbol{x}}^*$. It updates the seed points at 7. The location of the seed points will be updated as the cell having the lowest average distance with the other cells as suggested by Schneider et al. (2014).

That is, we set the seed point to be the point, which makes the sum distance between the cells assigned to the driver and this point to be the minimum. The algorithm resolves the DTP problem with the actual demand in Steps 9–10, which sets the core area assignment obtained in the STP stage as constraints. Then the algorithm updates the experience matrix in Step 11. Finally, it returns the optimal solution in Step 13.

5. Computational studies

In this section, we report on the numerical studies of our proposed territory planning method. We summarize the contents of the numerical studies in Table 1.

5.1. Experiment setup

We consider a service region of 150×150 units with the depot located at the center. For each case of the TPP, 20 instances are generated. The location of the cells is generated with uniform distribution Unif$(0, 150)$, and the demand of the cells is generated with Unif$(0, 5)$ if not otherwise stated. The uniform distributed customers is one of the most common assumptions adopted to test the performance of the territory planning algorithms (e.g., Lespay and Suchan, 2022; Sandoval et al., 2022). According to Zhong et al. (2007), the performance of the TPP algorithms is similar under different distributions. Note that, the capacity constraints, time window, and traffic congestion are not considered in the default case (i.e., $w_{1,2} = w_{1,3} = 0$), and we configure $w_{1,1} = 0.765$ following Stein (1978). The effects of these practical constraints are analyzed in Section 5.3. Without losing generality, flex zone is configured as 60% of the service region. The default parameters are $h = 7$ days, $I = 300$ cells, $T = 84$ days, and $K = 4$ drivers if

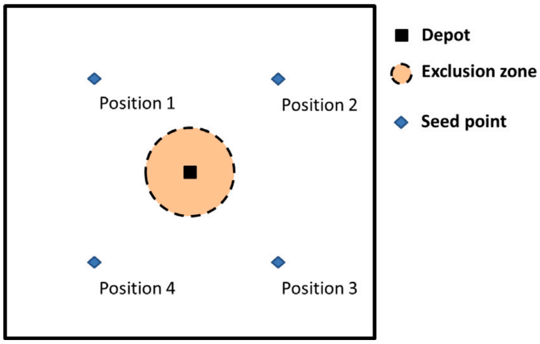

Fig. 4. Positions of the initial seed points.

Table 2
The performance of the TSRH method on the TPP with different computation interval.

h	$\bar{F}_2^*$	Runtime (s)		
		Max.	Min.	Avg.
7	5559.75	350.91	339.65	343.63
14	5559.80	336.57	333.43	334.37
21	5568.49	333.77	328.50	330.76
28	5567.58	332.49	330.61	331.78
35	5570.22	329.62	326.46	328.57
42	5574.55	331.79	319.79	323.63

Table 3
The performance of the TSRH method on the TPP with different number of drivers.

K	$\bar{F}_2^*$	Runtime (s)		
		Max.	Min.	Avg.
20	185 239.20	1627.11	1611.02	1618.85
25	173 550.87	1940.30	1918.60	1932.44
30	136 054.28	2227.17	2177.95	2204.97
35	122 657.15	2455.86	2442.25	2449.72
40	114 009.53	2766.47	2744.82	2755.92
45	78 867.61	3012.84	2992.99	3001.46
50	78 357.87	3365.36	3299.38	3331.08
55	74 052.31	3638.69	3624.29	3629.51

not otherwise mentioned. The initial seed points in Sections 5.2 to 5.5 are randomly generated from the cells outside the exclusion zone. In the studies in Sections 5.6 to 5.9. we have identified the properties with intensive numerical studies. We present these properties with the case with four drivers in the TPP, and the initial seed points are at coordinates $(40, 40)$, $(40, 110)$, $(110, 40)$, and $(110, 110)$ as illustrated in Fig. 4. For simplicity, we refer the drivers who have seed point at position $p \in \{1, 2, 3, 4\}$ as driver p. The seed points will be updated by the TSRH algorithm as discussed in Section 4.4.

In our study, all the algorithms are implemented in the Python 3.8 environment. We rely on the MILP solver Gurobi to solve the sub-problems. The experiments are performed on a computer with an Intel Core i9-10900K 3.7 GHz CPU and 64 GB of RAM.

5.2. Efficiency of the TSRH method

In this section, we provide a detailed analysis of the performance of the TSRH method. For each instance, we randomly generate the learning parameters α and β from the uniform distribution Unif$(0, 1)$ for all the drivers.

We begin by investigating the efficiency of the algorithm under different computation interval h with the default parameters. The results are presented in Table 2. In the table, $\bar{F}_2^*$ refers to the average optimal traveling time of the DTP among the T days.

We can tell from the table that the runtime is stable with different computation interval h, and the average optimal value is the minimum when $h = 7$. When the computation interval is small, the algorithm can utilize the latest information on the demand, and thus improve the performance of the drivers.

We then study the efficiency of the algorithm under different numbers of drivers. We consider the cases with $I = 2000$ cells and $K \in \{20, 25, \ldots, 55\}$ drivers. Because the runtime has little variance under different h suggested by Table 2, all the following computational studies in this section are conducted by configuring $h = 7$. We report the runtime of the TSRH algorithm on the TPP with different K in Table 3.

Table 4
The performance of the TSRH method on the TPP with different number of cells.

I	$\bar{F}_2^*$	Runtime (s)		
		Max.	Min.	Avg.
1000	31 914.58	1378.28	1373.61	1375.62
1500	107 370.19	2043.67	2034.88	2039.35
2000	113 688.80	2728.61	2713.00	2723.11
2500	285 465.23	3420.30	3392.89	3406.31
3000	315 341.60	4169.04	4141.29	4157.62

Table 5
The performance of the TSRH method on the TPP with different planning time.

T	$\bar{F}_2^*$	Runtime (s)		
		Max.	Min.	Avg.
70	197 605.07	1767.48	1756.11	1760.55
84	197 353.49	2083.59	2068.68	2078.60
98	196 661.74	2567.51	2522.04	2548.54
112	195 982.20	3028.31	2993.32	3010.90
126	195 756.45	3233.53	3182.94	3203.95
140	194 716.88	4082.84	4045.17	4065.70

We can tell from the table that, as the number of drivers (K) increases, the optimal value decreases. Because the value of total demand is relatively stable among all the instances and the drivers can work parallel for the delivery tasks, a larger group of drivers can reduce the average workload for a single driver. Therefore, the optimal traveling time is reduced when there are more drivers. On the other hand, the average runtime of the algorithm increases as K grows, because the size of the TPP increases. In addition, we find that the maximum and minimum runtime are close to each other. This reveals that the efficiency of our algorithm is quite robust under different situations.

Next, we investigate the efficiency of the algorithm in solving the TPP with different numbers of cells. We consider the case with $K = 40$ drivers and $I \in \{1000, 1500, \dots, 3000\}$ cells. We present the performance of the algorithm in Table 4.

We can tell from the above table, that the optimal value increases as the number of cells (I) grows. This is a natural result that the drivers take more time to finish the delivery tasks when there are more customers to serve. The runtime of the algorithm also increases as I grows, because the size of the TPP increases. The algorithm is still robust on the TPP with a given number of cells.

Fourth, we investigate the impact of planning time T on the efficiency of the algorithm. We consider the case with $K = 40$ drivers, $I = 1500$ cells, and $T \in \{70, 84, \dots, 140\}$ days. The performance of the algorithm is shown in Table 5.

We can tell that the runtime increases dramatically as T grows, because the size of the TPP grows to make the TPP more complex to resolve. On the other hand, the average optimal value decreases as the planning time grows. This is caused by the learning effect. The drivers have a longer time to learn from the working experience and optimize their delivery tasks when T is larger. Therefore, the optimal traveling time decreases as T grows.

5.3. Sensitivity analysis with practical constraints

In this section, we investigate the effects of the transportation uncertainty and capacity constraints on the territory plan.

5.3.1. Transportation uncertainty

First, we analyze the effects of transportation uncertainty on the traveling time of the drivers. The transportation uncertainty includes time-window constraints and traffic congestion in the operations and delivery. Let p_u be the transportation uncertainty level, which is given by:

$$p_u = \frac{\sum_{i\in\mathcal{I},t\in\mathcal{T}} n'_{i,t}}{\sum_{i\in\mathcal{I},t\in\mathcal{T}} n_{i,t}} \cdot 100\%. \tag{28}$$

We take the default parameters and investigate the changes in the traveling time as the transportation uncertainty level grows, where $p_u \in \{0, 20\%, 40\%, 60\%, 80\%, 100\%\}$. We have analyzed the properties of the traveling time with intensive numerical studies. To better present the trend of the changes with p_u increasing, we report the traveling time of five randomly generated cases in Table 6.

The results show that the traveling time increases monotonically as the uncertainty level (p_u) grows. When the drivers serve the customers having unexpected events, it takes the driver multiple visits or more time to finish the delivery tasks. Thus, the traveling time is higher when p_u is large.

Table 6
The effects of transportation uncertainty on territory design efficiency.

p_u	$\bar{F}_2^*$				
	Case 1	Case 2	Case 3	Case 4	Case 5
0%	6120.35	7642.48	6460.55	6464.82	7196.19
20%	6128.06	7805.88	6485.94	6485.98	7203.19
40%	6135.67	7813.05	6530.48	6562.98	7210.16
60%	6163.64	7819.01	6800.95	6770.08	7217.17
80%	6171.30	7838.76	7037.46	6877.35	7224.04
100%	6176.90	7848.12	7122.60	6984.41	7231.03

Table 7
The effects of vehicle capacity on territory design efficiency.

p_c	$\bar{F}_2^*$				
	Case 1	Case 2	Case 3	Case 4	Case 5
20%	6230.75	7858.23	6593.62	6548.20	7279.88
40%	6184.58	7855.71	6529.77	6391.96	7238.04
60%	6171.31	7839.00	6508.12	6377.56	7224.09
80%	6163.60	7820.71	6501.07	6370.36	7217.11
100%	6158.98	7816.08	6497.86	6366.03	7212.93

5.3.2. *Capacity constraints*

Next, we discuss the effect of vehicle capacity constraints on dispatch efficiency. As defined in Section 3.1, each driver has a maximum working time b_k. Let p_c be the capacity level with regard to b_k, which is given by:

$$p_c = \frac{\mu_k}{b_k} \cdot 100\%, \forall k \in \mathcal{K}. \tag{29}$$

We then investigate the changes in the traveling time as the capacity level grows with the default parameters, where $p_c \in \{20\%, 40\%, 60\%, 80\%, 100\%\}$. Similarly, the traveling time with five randomly generated cases are reported to illustrate the trend in the changes of traveling time. The results can found in Table 7.

We can see from Table 7 that the traveling time decreases monotonically as the capacity level grows. When the drivers have higher capacity, they can finish the delivery tasks within less number of journeys. Therefore, the traveling time decreases in p_c.

5.4. *Random errors in the transportation estimation*

In our study, we build the TSRH algorithm based on the transportation time approximation methods in Daganzo (1984) and Figliozzi (2009). According to Figliozzi (2009), the estimation method performs well under various conditions, but the precision of the estimation is affected by random errors in practice. Given that the random errors are unavoidable, we then investigate the effect of the random errors on the optimal territory plan with numerical experiments.

Let Γ be the variable of the random error. By Figliozzi (2009), the estimation method has an error of less than 5%. Thus, we assume that Γ follows the uniform distribution Unif$(-0.05, 0.05)$. The estimated transportation time in (10) and (11) is affected by the random error, and it is given by:

$$C'_{i,k,t}(\rho_{i,k,t}, \bar{n}_{i,t}, \bar{n}'_{i,t}, \mu_k) = C_{i,k,t}(\rho_{i,k,t}, \bar{n}_{i,t}, \bar{n}'_{i,t}, \mu_k) \cdot (1 + \gamma_t), \tag{30}$$

$$D'_{i,k,t}(\rho_{i,k,t}) = D_{i,k,t}(\rho_{i,k,t}) \cdot (1 + \gamma_t), \tag{31}$$

where $C'_{i,k,t}(\rho_{i,k,t}, \bar{n}_{i,t}, \bar{n}'_{i,t}, \mu_k)$ and $D'_{i,k,t}(\rho_{i,k,t})$ are the estimated intra- and inter-cell transportation time with error γ_t at day t.

Let p_r be the relative gap between the daily transportation time with and without the random error, and it is given by:

$$p_r = \frac{\bar{F}_2^{*\prime\prime} - \bar{F}_2^*}{\bar{F}_2^*} \cdot 100\%, \tag{32}$$

where $\bar{F}_2^{*\prime\prime}$ and $\bar{F}_2^*$ are the optimal daily transportation time with and without random error.

We analyze the effects of the random error on the optimal transportation time with extensive numerical studies and present the results in Table 8 with 20 randomly generated cases. Let $\bar{\gamma}$ be the average random error during the T days in each case. We report both $\bar{\gamma}$ and p_r in the numerical study.

We can tell from the table that the accuracy of the transportation estimation varies in different cases. Since the random error in each day (γ_t) is generated by the uniform distribution Unif$(-0.05, 0.05)$, the average of the random error approaches the mean of Unif$(-0.05, 0.05)$, which is zero. In general, the relative gap p_r follows the trend of the average random error $\bar{\gamma}$. This fits the intuition that the accuracy of the estimation method grows when the random error decreases. We can also find that the relative gap is less than 0.5% in all the cases, which indicates the daily transportation time is affected by the random error only on a small scale.

Table 8
The effects of the random errors on the transportation time estimation.

Case	$\bar{\gamma}$	$\bar{F}_2^*$	$\bar{F}_2^{*''}$	p_r	case	$\bar{\gamma}$	$\bar{F}_2^*$	$\bar{F}_2^{*''}$	p_r
1	−0.0042	3439.99	3425.01	−0.435%	11	0.0008	3351.58	3354.20	0.078%
2	−0.0026	6240.71	6223.60	−0.274%	12	0.0011	4633.10	4638.40	0.114%
3	−0.0025	3329.69	3322.00	−0.231%	13	0.0014	3784.66	3788.67	0.106%
4	−0.0019	4204.91	4196.93	−0.190%	14	0.0015	5948.88	5959.49	0.178%
5	−0.0011	5026.11	5016.51	−0.191%	15	0.0020	3818.28	3827.98	0.254%
6	−0.0010	5294.81	5304.39	0.181%	16	0.0021	3416.28	3425.71	0.276%
7	−0.0008	3154.44	3150.10	−0.137%	17	0.0023	4020.24	4031.65	0.284%
8	−0.0001	4221.51	4222.53	0.024%	18	0.0026	4123.28	4137.43	0.343%
9	0.0002	3576.87	3575.45	−0.040%	19	0.0035	3619.44	3632.75	0.368%
10	0.0006	4199.19	4201.25	0.049%	20	0.0040	3264.79	3277.33	0.384%

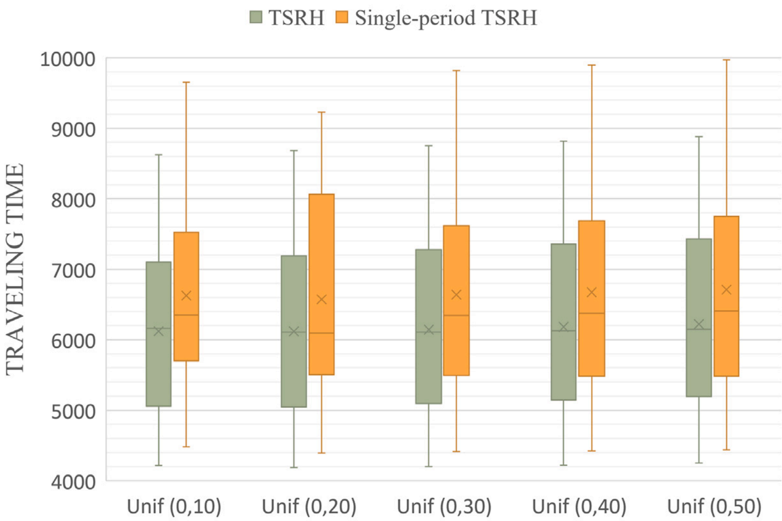

Fig. 5. Performance comparison between the TSRH and the single-period TSRH.

Due to the stochastic nature in the daily delivery operation, it is impossible to obtain a perfect estimation without errors. Yet, we can improve transportation estimation's precision by analyzing historical delivery data. The delivery service provider can examine the transportation time and calibrate the estimation parameters with regression (Figliozzi, 2009), which further enhances the performance of the estimation method.

5.5. The effects of using the periodical predicted data

In the classical territory planning literature (e.g., Zhong et al., 2007; Schneider et al., 2014), the territory planning algorithm does not apply the periodical predicted demand data in making the territory plans. The territory plan is computed one time with the data in the initial period. Differently, our algorithm allows the territory plans to be adjusted based on the latest prediction periodically, which can be more accurate. In this section, we investigate the effects of using periodical predicted demand data in computing the territory plans. We compare our TSRH algorithm with a single-period TSRH with $h = T$. We take the default parameters stated in Section 5.1 in the simulation, The results are shown in Fig. 5.

We can tell from the figure that the TSRH method can offer better solutions than the single-period TSRH method with a smaller average optimal traveling time $\bar{F}_2^*$. The computation time of the two methods is 345.67 s and 344.02 s, respectively. Because the TSRH method can apply the predicted demands in adjusting the core areas, the solutions are much better than the ones obtained from the single-period TSRH method. In addition, as the range of the demand increases, $\bar{F}_2^*$ shows an increasing trend. One possible explanation is that the drivers spend more time conducting the delivery to meet the increased demand.

5.6. The effects of the seed point updating methods

Intuitively, the choice of the seed points plays an important role as their location affects the assignment of the core area. By dividing the service region into four equally-sized sub-areas, the experiment above picks the cell having a minimum average distance to the other cells as the seed point in each sub-area. For comparison purposes, two other methods are proposed, i.e., picking the cell having minimum weighted sum distance to the other cells, where the weight is the demand in each cell, as the seed point, and

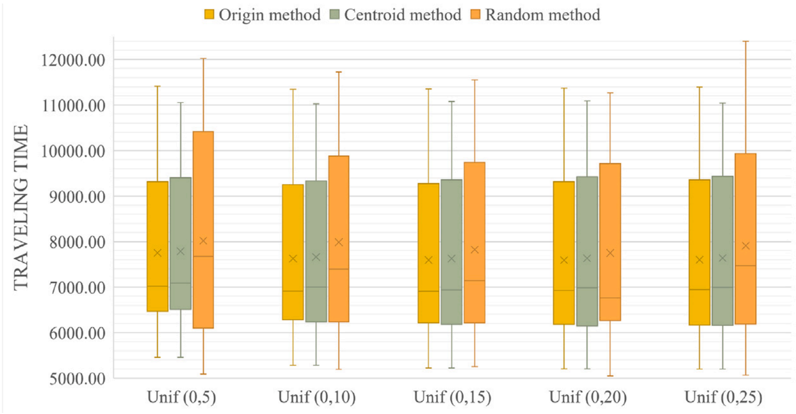

Fig. 6. The effect of different seed points updating methods on territory design.

picking a random cell as the seed point. The results are illustrated in Fig. 6, and methods are denoted as "origin method", "centroid method" and "random method". Similarly, each method is tested with the same 20 randomly generated cases for a fair comparison.

According to the box plot, the origin method is slightly better than the centroid and random methods, although the random method may have some outliers. So as long as the seed point is picked around a center position, the results will not vary significantly. In addition, the computation time of the three methods is nearly the same since the size of the TPP is identical.

5.7. Performance comparison with the Tabu search

In the TSRH algorithm we use the traveling time estimation to convert the TPP into MILPs and solve them by the commercial solver, while the TSTP algorithms apply Tabu Search to solve traveling salesman problem for the solution of subproblems (e.g., Zhong et al., 2007; Schneider et al., 2014). As we cannot compare the algorithms directly because the algorithms use different data (as we discussed in Section 5.5) and computation methods, we compare our TSRH algorithm with the modified TSRH using Tabu Search solving the DTPs. The framework of the Tabu Search is discussed in Appendix C.

We conduct the numerical studies with default parameters lasting $T \in \{70, 84, \ldots, 126\}$ days. The parameters of the Tabu Search include stopping criteria $\Delta = 10000$, and length of the tabulist $\sigma = 50$. We analyze the gap of the optimal traveling time between the TSRH algorithm and the Tabu Search. Let the gap be p_g, and it is given by:

$$p_g = \frac{\bar{F}_2^{*\prime} - \bar{F}_2^*}{\bar{F}_2^*} \times 100\%. \tag{33}$$

where $\bar{F}_2^*$ is the optimal value computed by the TSRH algorithm and $\bar{F}_2^{*\prime}$ is the optimal value provided by the TSRH with Tabu Search.

We analyze the changes in traveling time with insensitive numerical studies, and report five randomly generated cases to illustrate the efficiency of the algorithms in Table 9.

We can tell from the table that the optimal travel time computed by the TSRH algorithm is smaller than the TSRH with Tabu Search for all five cases. The gap of the optimal value is around 6%. The TSRH algorithm can generate better solutions than the Tabu Search under different planning times T.

5.8. Territory planning with homogeneous drivers

In this section, we discuss the impact of the learning effect on the territory design with a homogeneous group of drivers. We investigate the impact of both the learning potential parameter α and the learning efficiency parameter β. We assume each parameter falls into three categories, which are "high", "medium", and "low", as suggested by Chen et al. (2016). Following Dar-El (2013), we introduce $\alpha \in \{0.1, 0.3, 0.5\}$, which stands for low, medium, and high learning potential, and introduce $\beta \in \{0.2, 0.4, 0.6\}$, which stands for low, medium, and high learning efficiency respectively.

We start by analyzing the effect of learning potential on the traveling time of the drivers. Assuming that all the drivers have medium-level learning efficiency (i.e., $\beta = 0.4$), we present the optimal traveling time under different learning potential in Fig. 7.

We can tell from Fig. 7(a), when $\alpha = 0.1$, the drivers only have a small fraction of traveling time that can be compressed by the learning effect. The traveling time changes dramatically before day 14, but it then turns stable. All the drivers have a similar pattern, and the variance of the traveling time is very high. The traveling time of a driver on the last day is around 1850 units. When the drivers have high learning potential (i.e., when $\alpha = 0.5$), we can tell from Fig. 7(c) that the traveling time changes greatly. The traveling time of a driver on the last day is around 1150 units, and it changes more smoothly with less variance than Fig. 7(a).

Table 9
Performance comparison with the Tabu Search.

T		Case 1	Case 2	Case 3	Case 4	Case 5	Avg. Value
70	$\bar{F}_2^*$	4190.05	7986.26	5743.89	7279.62	5229.42	6085.85
	$\bar{F}_2^{*'}$	4504.85	8662.03	6114.54	7539.68	5540.88	6472.40
	Gap	7.51%	8.46%	6.45%	3.57%	5.96%	6.39%
84	$\bar{F}_2^*$	4146.37	7963.55	5656.95	7245.88	5169.80	6036.51
	$\bar{F}_2^{*'}$	4452.60	8635.87	6015.40	7502.03	5457.64	6412.71
	Gap	7.39%	8.44%	6.33%	3.54%	5.57%	6.25%
98	$\bar{F}_2^*$	4116.77	7942.99	5586.77	7218.19	5111.94	5995.33
	$\bar{F}_2^{*'}$	4416.03	8617.12	5942.51	7476.45	5398.43	6370.11
	Gap	7.26%	8.49%	6.37%	3.58%	5.60%	6.26%
112	$\bar{F}_2^*$	4091.84	7922.84	5541.78	7198.56	5073.44	5965.69
	$\bar{F}_2^{*'}$	4388.00	8596.78	5890.21	7456.01	5352.01	6336.60
	Gap	7.23%	8.51%	6.29%	3.58%	5.49%	6.22%
126	$\bar{F}_2^*$	4073.60	7908.82	5502.56	7187.88	5042.80	5943.13
	$\bar{F}_2^{*'}$	4371.52	8582.98	5848.54	7435.16	5317.07	6311.05
	Gap	7.31%	8.52%	6.29%	3.44%	5.44%	6.20%

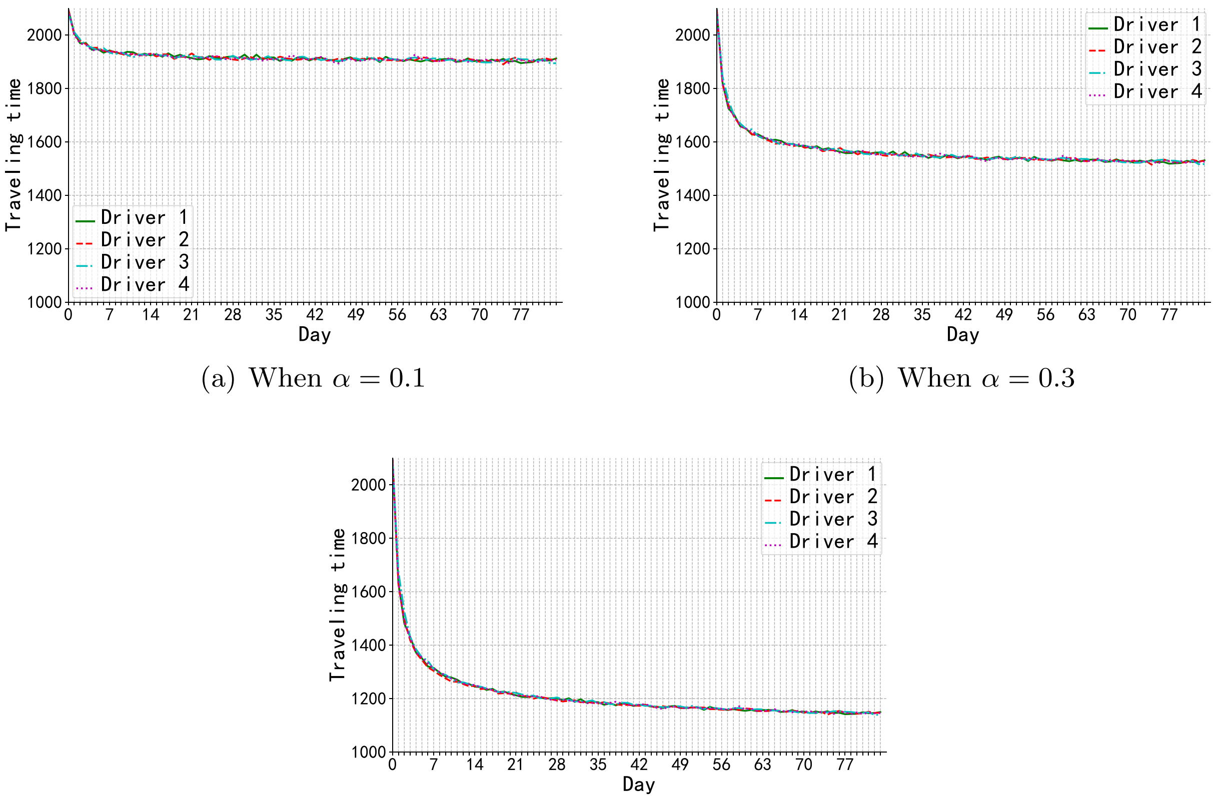

(a) When $\alpha = 0.1$ (b) When $\alpha = 0.3$ (c) When $\alpha = 0.5$

Fig. 7. Change of the traveling time under different learning potential.

By the end of the medium potential case, the driver's traveling time is reduced to a medium level. We can tell that the traveling time changes more smoothly when the learning potential is higher.

Next, we investigate the effect of learning efficiency. Assuming that all the drivers have medium-level learning potential (i.e., $\alpha = 0.3$), we present the optimal traveling time under different learning efficiency in Fig. 8.

We can tell from Fig. 8(a), when $\beta = 0.2$, the drivers have a low speed to reduce the traveling time, and it changes almost in a linear trend. The traveling time of a driver by the end is around 1650 units. When the drivers have a high learning efficiency (i.e., when $\beta = 0.6$), we can tell from Fig. 8(c) that the drivers' traveling time reduces quickly. The traveling time of a driver by the

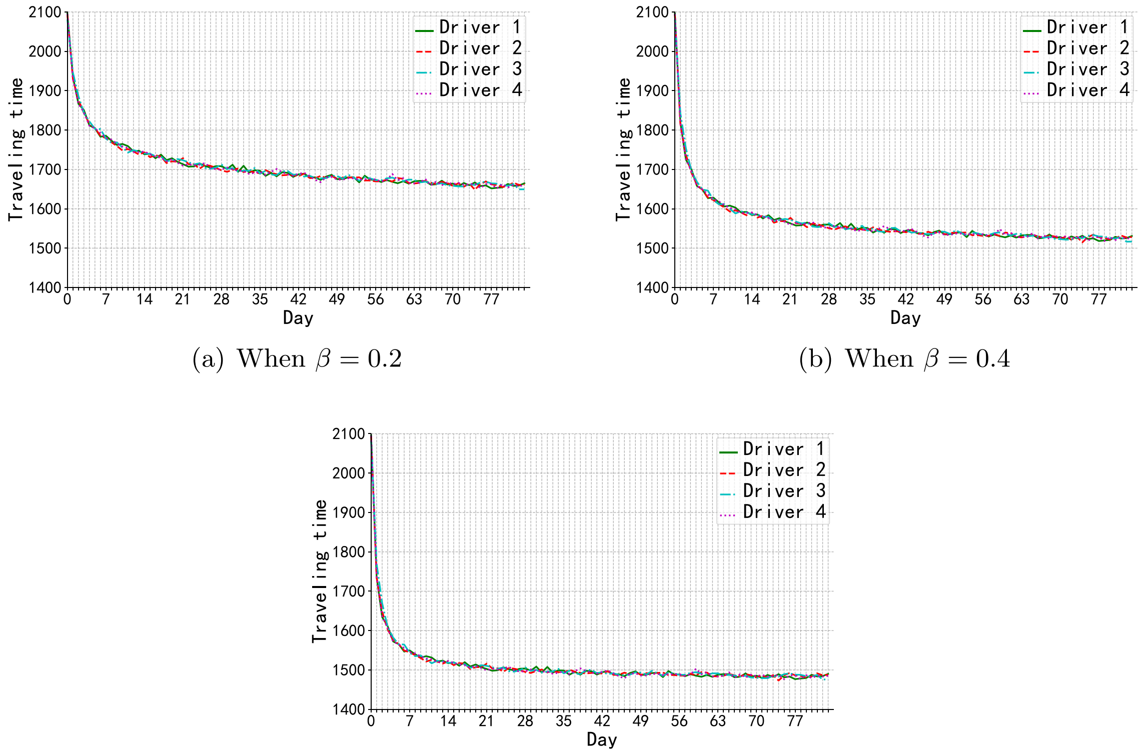

(a) When $\beta = 0.2$

(b) When $\beta = 0.4$

(c) When $\beta = 0.6$

Fig. 8. Change of the traveling time under different learning efficiency.

Table 10
Configurations of the numerical studies on heterogeneous drivers.

Configuration	Case	Learning parameter of the drivers	
		α	β
Heterogeneous learning potential	1	0.5, 0.5, 0.5, 0.1	0.4, 0.4, 0.4, 0.4
	2	0.1, 0.1, 0.1, 0.5	0.4, 0.4, 0.4, 0.4
Heterogeneous learning efficiency	3	0.3, 0.3, 0.3, 0.3	0.6, 0.6, 0.6, 0.2
	4	0.3, 0.3, 0.3, 0.3	0.2, 0.2, 0.2, 0.6

end is around 1500 units, and the curve turns stable after day 28. By Fig. 8(b), we can see that the traveling time is compressed to the medium level when the drivers have a medium learning efficiency parameter.

5.9. Territory planning with heterogeneous drivers

In this section, we investigate the impact of the learning effect with a heterogeneous group of drivers. Following Section 5.8, we investigate the effects of both learning potential and learning efficiency, which fall into the three categories. To facilitate the analysis, we control three of the four drivers to have homogeneous learning capabilities and assume the other driver has different learning parameters from these three drivers. The configurations of the numerical studies are presented in Table 10

We consider four cases of heterogeneous drivers. In the first two cases, drivers have heterogeneous learning potential, while the learning potential of the drivers is homogeneous in cases 3 and 4. Driver 4 has low learning potential in case 1, and high learning potential in case 2. In addition, driver 4 has low learning efficiency in case 3 and high learning efficiency in case 4.

5.9.1. Heterogeneous learning potential

In this section, we analyze the case when the drivers have heterogeneous learning potential. We compare the changes in the territory size and territory plan in Fig. 9.

We can tell from Fig. 9(a) because driver 4 has the least learning potential, fewer cells are assigned to him after day 63. Some cells are reassigned to other drivers who have higher learning potential. Fig. 9(b) shows the change of traveling time of each driver. Driver 4 has the highest traveling time since he has the least learning potential. The traveling time of driver 4 drops when the other drivers take some cells from him.

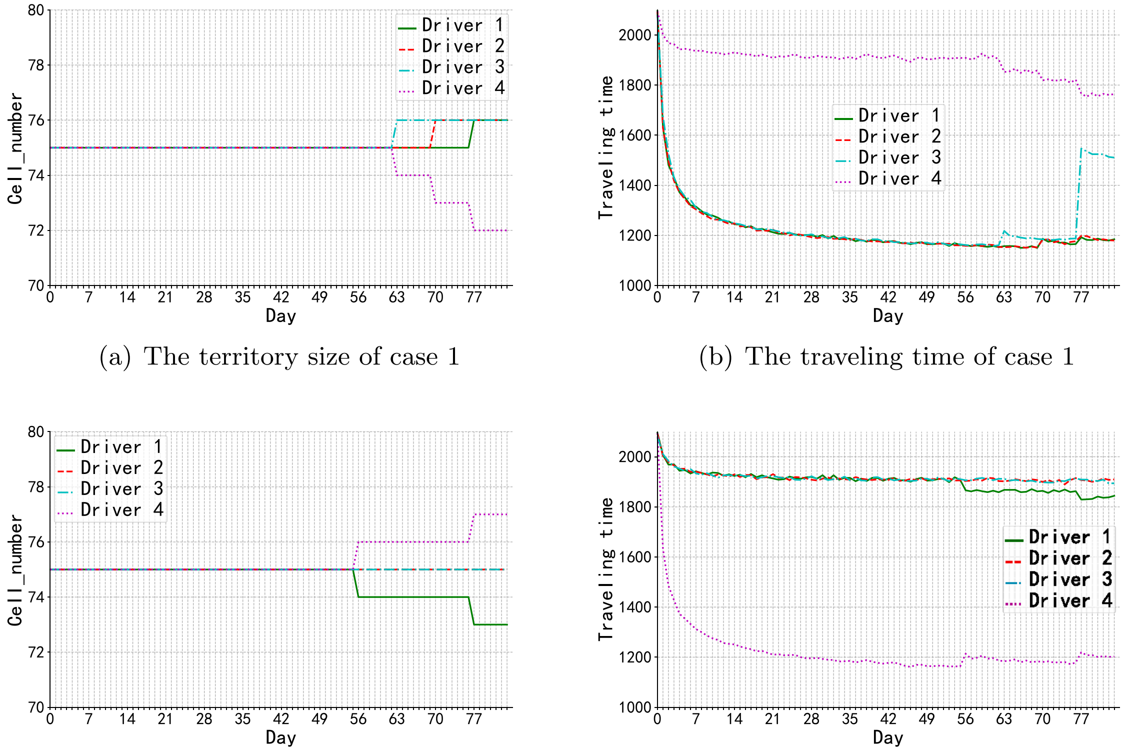

(a) The territory size of case 1

(b) The traveling time of case 1

(c) The territory size of case 2

(d) The traveling time of case 2

Fig. 9. Changes in the territory size and traveling time in the cases with heterogeneous learning potential.

When driver 4 has the highest learning potential, we can tell from Fig. 9(c) that the number of cells assigned to driver 4 increases, and the number of cells assigned to driver 1 decreases. Driver 4 is assigned with some other cells to make full use of his capability. In addition, as Fig. 9(d) illustrates, the traveling time of driver 4 is the lowest since he has the largest learning potential.

5.9.2. Heterogeneous learning efficiency

In this section, we study the impact of heterogeneous learning efficiency. We present the changes of territory size and traveling time in Fig. 10.

We can tell from Fig. 10(a), the size of driver 4's territory decreases after day 70, while the size of other drivers' territories increases because driver 4 has the least learning efficiency. Fig. 10(b) shows that driver 4's traveling time is higher than the other three drivers'. While each driver's traveling time decreases, there are several spikes in the traveling time in Fig. 10(b). The spike appears each time that the territory design changes. When a driver obtains new cells, it takes more time for the new tasks, but when he gets familiar with the cells, the traveling time drops again.

When driver 4 has the highest learning efficiency, as is shown in Fig. 10(c), the size of driver 4's territory increases, while drivers 1 and 3's territory size decreases. Driver 4 takes multiple cells from drivers 1 and 3, and driver 2's territory remains unchanged. An explanation of the phenomenon is the geographic topology of the drivers. Drivers 1, and 3 are closer to driver 4, such that their cells are transferred to driver 4 first. Fig. 10(d), verifies that driver 4 can learn at the highest efficiency among the drivers. His traveling time decreases fast at the beginning and remains stable after day 42.

We can see that the territory size and the traveling time change differently in the four cases. The learning capabilities have different effects on the optimal territory design. Comparing Figs. 9 and 10, we can find that learning potential would affect the amount of time that can be compressed and the learning efficiency would affect the speed of the time being compressed. The traveling time in Fig. 9 turns stable after a certain time period, while the traveling time keeps reducing in Fig. 10. In all cases, cells can be transferred to the high-capability drivers after a few working days. Even though a sudden change in the traveling time may occur when a driver loses or obtains new cells, the driver can soon adapt to the new task and the delivery efficiency improves by the learning effect. Finally, learning potential and learning efficiency can have different effects on the traveling time.

6. Conclusion

To survive in the highly competitive industry, the delivery service providers have adopted various technologies and methods to improve the service experience. The territory-based delivery system is frequently used to conduct the delivery, in which the

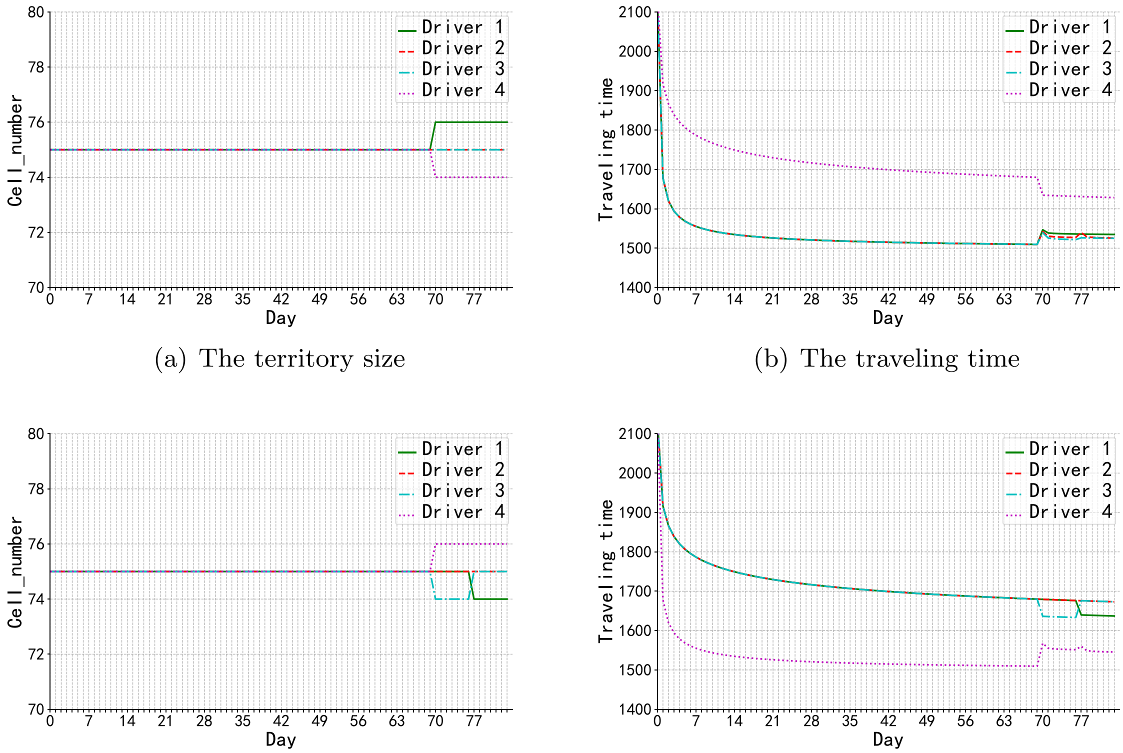

(a) The territory size (b) The traveling time

(c) The territory size (d) The traveling time

Fig. 10. Changes in the territory size and traveling time of case 3.

service region is divided into several territories served by the couriers. The advantage is that the system can enhance the service consistency, but the territory plan can be outdated as the demand and experience change. In this paper, we build up an MDP model for the territory design and vehicle dispatching problem. We consider an exponential learning process, which considers both the potential and efficiency to reduce the travel time by the learning. We propose a TSRH algorithm to resolve the TPP. In the first stage, part of the cells is assigned to the drivers as core areas by the predicted demands. In the second stage, the remaining cells are assigned to the drivers by the actual demands. Numerical studies suggest that the proposed TSRH algorithm can resolve the TPP efficiently and it is robust under different situations. The TSRH method is proved to be able to offer better solutions than the TSTP method in Zhong et al. (2007). Furthermore, our study suggests that the learning effect can largely impact the territory design and the optimal traveling time.

In our research, we do not consider the time window constraints because we consider the situation where the package stations and express cabinets are used. In practice, time-window may still need to be considered for the region that the package station and express cabinet are not introduced. One research direction is to develop an algorithm to resolve the TPP with time-window constraints. On another hand, there may be different types of customers in the same area (e.g., commercial and individual customers). The customers may act differently, and the drivers' delivery experience may also accumulate differently when dealing with these customers. Another avenue of future research is to consider the customer heterogeneity in the TPP and study the optimal territory design. Finally, it would be interesting to discuss the application of reinforcement learning or approximate dynamic programming in solving the TPP.

CRediT authorship contribution statement

Yifu Li: Methodology, Investigation, Validation, Writing – original draft, Writing – review & editing, Supervision. **Chenhao Zhou:** Conceptualization, Methodology, Investigation, Validation, Writing – original draft, Writing – review & editing, Supervision, Funding acquisition. **Peixue Yuan:** Software, Formal analysis, Investigation, Writing – review & editing. **Thi Tu Anh Ngo:** Software, Visualization.

Declaration of competing interest

The authors declare that they have no known competing financial interests or personal relationships that could have appeared to influence the work reported in this paper.

Data availability

No data was used for the research described in the article.

Acknowledgments

This research is supported by the National Natural Science Foundation of China [72201210, 72101203], Shaanxi Provincial Key R&D Program, China [2022KW-02], and The Youth Innovation Team of Shaanxi Universities, China.

Appendix A. Supplementary data

Supplementary material related to this article can be found online at https://doi.org/10.1016/j.tre.2023.103036.

References

Bailey, C.D., 1989. Forgetting and the learning curve: A laboratory study. Manage. Sci. 35 (3), 340–352.
Beardwood, J., Halton, J.H., Hammersley, J.M., 1959. The shortest path through many points. Math. Proc. Camb. Phil. Soc. 55 (4), 299–327.
Beasley, J., 1984. Fixed routes. J. Oper. Res. Soc. 35 (1), 49–55.
Bender, M., Meyer, A., Kalcsics, J., Nickel, S., 2016. The multi-period service territory design problem–an introduction, a model and a heuristic approach. Transp. Res. E 96, 135–157.
Chang, T.-S., Yen, H.-M., 2012. City-courier routing and scheduling problems. European J. Oper. Res. 223 (2), 489–498.
Chen, X., Thomas, B.W., Hewitt, M., 2016. The technician routing problem with experience-based service times. Omega 61, 49–61.
Chen, X., Thomas, B.W., Hewitt, M., 2017. Multi-period technician scheduling with experience-based service times and stochastic customers. Comput. Oper. Res. 82, 1–14.
Chopra, S., Meindl, P., 2016. Supply Chain Management, Strategy, Planning, and Operation. Pearson, New York, NY, USA.
Cook, R.A., Lodree, E.J., 2017. Dispatching policies for last-mile distribution with stochastic supply and demand. Transp. Res. E 106, 353–371.
Daganzo, C.F., 1984. The distance traveled to visit N points with a maximum of C stops per vehicle: An analytic model and an application. Transp. Sci. 18 (4), 331–350.
Dar-El, E.M., 2013. Human Learning: From Learning Curves to Learning Organizations, Vol. 29. Springer Science & Business Media, New York.
De Jong, J., 1957. The effects of increasing skill on cycle time and its consequences for time standards. Ergonomics 1 (1), 51–60.
Dong, Z., Turnquist, M.A., 2015. Combining service frequency and vehicle routing for managing supplier shipments. Transp. Res. E 79, 231–243.
Figliozzi, M.A., 2009. Planning approximations to the average length of vehicle routing problems with time window constraints. Transp. Res. B 43 (4), 438–447.
Glock, C.H., Grosse, E.H., Jaber, M.Y., Smunt, T.L., 2019. Applications of learning curves in production and operations management: A systematic literature review. Comput. Ind. Eng. 131, 422–441.
Groër, C., Golden, B., Wasil, E., 2009. The consistent vehicle routing problem. Manuf. Serv. Oper. Manag. 11 (4), 630–643.
Hewitt, M., Chacosky, A., Grasman, S.E., Thomas, B.W., 2015. Integer programming techniques for solving non-linear workforce planning models with learning. European J. Oper. Res. 242 (3), 942–950.
Huang, Y., Savelsbergh, M., Zhao, L., 2018. Designing logistics systems for home delivery in densely populated urban areas. Transp. Res. B 115, 95–125.
Jaber, M.Y., 2016. Learning Curves: Theory, Models, and Applications. CRC Press, New York.
Jaber, M.Y., Glock, C.H., 2013. A learning curve for tasks with cognitive and motor elements. Comput. Ind. Eng. 64 (3), 866–871.
Karmarkar, U., 2015. OM forum—the service and information economy: Research opportunities. Manuf. Serv. Oper. Manag. 17 (2), 136–141.
Kovacs, A.A., Golden, B.L., Hartl, R.F., Parragh, S.N., 2015. The generalized consistent vehicle routing problem. Transp. Sci. 49 (4), 796–816.
Kumar, P., Baraiya, R., Das, D., Jakhar, S.K., Xu, L., Mangla, S.K., 2021. Social responsibility and cost-learning in dyadic supply chain coordination. Transp. Res. E 156, 102549.
Laporte, G., 1992. The vehicle routing problem: An overview of exact and approximate algorithms. European J. Oper. Res. 59 (3), 345–358.
Larson, R.C., Odoni, A.R., 1981. Urban Operations Research. Prentice-Hall, New Jersey.
Lee, E., Cen, X., Lo, H.K., 2021. Zonal-based flexible bus service under elastic stochastic demand. Transp. Res. E 152, 102367.
Lespay, H., Suchan, K., 2022. Territory design for the multi-period vehicle routing problem with time windows. Comput. Oper. Res. 145, 105866.
Mazur, J.E., Hastie, R., 1978. Learning as accumulation: A re-examination of the learning curve. Psychol. Bull. 85 (6), 1256.
Nicola, D., Vetschera, R., Dragomir, A., 2019. Total distance approximations for routing solutions. Comput. Oper. Res. 102, 67–74.
Pei, M., Lin, P., Du, J., Li, X., Chen, Z., 2021. Vehicle dispatching in modular transit networks: A mixed-integer nonlinear programming model. Transp. Res. E 147, 102240.
Quirion-Blais, O., Chen, L., 2021. A case-based reasoning approach to solve the vehicle routing problem with time windows and drivers' experience. Omega 102, 102340.
Redelmeier, D.A., Kahneman, D., 1996. Patients' memories of painful medical treatments: Real-time and retrospective evaluations of two minimally invasive procedures. Pain 66 (1), 3–8.
Sandoval, M.G., Álvarez-Miranda, E., Pereira, J., Ríos-Mercado, R.Z., Díaz, J.A., 2022. A novel districting design approach for on-time last-mile delivery: An application on an express postal company. Omega 113, 102687.
Schneider, M., Stenger, A., Schwahn, F., Vigo, D., 2014. Territory-based vehicle routing in the presence of time-window constraints. Transp. Sci. 49 (4), 732–751.
Smilowitz, K., Nowak, M., Jiang, T., 2013. Workforce management in periodic delivery operations. Transp. Sci. 47 (2), 214–230.
Stein, D.M., 1978. An asymptotic, probabilistic analysis of a routing problem. Math. Oper. Res. 3 (2), 89–101.
Ulmer, M., Nowak, M., Mattfeld, D., Kaminski, B., 2020. Binary driver-customer familiarity in service routing. European J. Oper. Res. 286 (2), 477–493.
Valeva, S., Hewitt, M., Thomas, B.W., 2017. A matheuristic for workforce planning with employee learning and stochastic demand. Int. J. Prod. Res. 55 (24), 7380–7397.
Wong, K., Beasley, J.E., 1984. Vehicle routing using fixed delivery areas. Omega 12 (6), 591–600.
Zhang, J., Liu, F., Tang, J., Li, Y., 2019. The online integrated order picking and delivery considering Pickers' learning effects for an O2O community supermarket. Transp. Res. E 123, 180–199.
Zhang, G., Smilowitz, K., Erera, A., 2011. Dynamic planning for urban drayage operations. Transp. Res. E 47 (5), 764–777.
Zhong, H., Hall, R.W., Dessouky, M., 2007. Territory planning and vehicle dispatching with driver learning. Transp. Sci. 41 (1), 74–89.

Dr. Yifu Li is a Tenure-Track Associate Professor at the School of Management, University of Science and Technology of China. He obtained his Ph.D. in Industrial Engineering and Logistics Management from the Hong Kong University of Science and Technology in 2018. After graduation, he worked at National University of Singapore and Xi'an JiaotongLiverpool University. His research interests are behavioral scheduling and decisions.

Dr. Chenhao Zhou is a Professor from School of Management in Northwestern Polytechnical University. Prior to this, he was a Research Assistant Professor in the Department of Industrial Systems Engineering and Management, National University of Singapore. His research interests are transportation systems and maritime logistics using simulation and optimization methods.

Peixue Yuan, is a Master student from School of Management in Northwestern Polytechnical University.

Thi Tu Anh Ngo is a research assistant of Department of Industrial Systems Engineering and Management in National University of Singapore.